Environmental Technology

ISSN: 0959-3330 (Print) 1479-487X (Online) Journal homepage: https://www.tandfonline.com/loi/tent20

Combining activated carbon adsorption with heterogeneous photocatalytic oxidation: Lack of synergy for biologically treated greywater and tetraethylene glycol dimethyl ether

Holger Gulyas , Ángel Santiago Oria Argáez , Fanzhuo Kong , Carlos Liriano Jorge , Susanne Eggers & Ralf Otterpohl

To cite this article: Holger Gulyas , Ángel Santiago Oria Argáez , Fanzhuo Kong , Carlos Liriano Jorge , Susanne Eggers & Ralf Otterpohl (2013) Combining activated carbon adsorption with heterogeneous photocatalytic oxidation: Lack of synergy for biologically treated greywater and tetraethylene glycol dimethyl ether, Environmental Technology, 34:11, 1393-1403, DOI: 10.1080/09593330.2012.751129

To link to this article: https://doi.org/10.1080/09593330.2012.751129

Published online: 04 Jan 2013.

Environmental Technology, 2013
Vol. 34, No. 11, 1393–1403, http://dx.doi.org/10.1080/09593330.2012.751129

Taylor & Francis
Taylor & Francis Group

Combining activated carbon adsorption with heterogeneous photocatalytic oxidation: Lack of synergy for biologically treated greywater and tetraethylene glycol dimethyl ether

Holger Gulyas*, Ángel Santiago Oria Argáez, Fanzhuo Kong, Carlos Liriano Jorge, Susanne Eggers and Ralf Otterpohl

Institute of Wastewater Management and Water Protection, Hamburg University of Technology, Hamburg, Germany

(*Received 4 May 2012: final version received 15 November 2012*)

The aim of the study was to evaluate whether the addition of activated carbon in the photocatalytic oxidation of biologically pretreated greywater and of a polar aliphatic compound gives synergy, as previously demonstrated with phenol. Photocatalytic oxidation kinetics were recorded with fivefold concentrated biologically pretreated greywater and with aqueous tetraethylene glycol dimethyl ether solutions using a UV lamp and the photocatalyst TiO_2 P25 in the presence and the absence of powdered activated carbon. The synergy factor, SF, was quantified as the ratio of photocatalytic oxidation rate constant in the presence of powdered activated carbon to the rate constant without activated carbon. No synergy was observed for the greywater concentrate ($SF \approx 1$). For the aliphatic compound, tetraethylene glycol dimethyl ether, addition of activated carbon actually had an inhibiting effect on photocatalysis ($SF < 1$), while synergy was confirmed in reference experiments using aqueous phenol solutions. The absence of synergy for the greywater concentrate can be explained by low adsorbability of its organic constituents by activated carbon. Inhibition of the photocatalytic oxidation of tetraethylene glycol dimethyl ether by addition of powdered activated carbon was attributed to shading of the photocatalyst by the activated carbon particles. It was assumed that synergy in the hybrid process was limited to aromatic organics. Regardless of the lack of synergy in the case of biologically pretreated greywater, the addition of powdered activated carbon is advantageous since, due to additional adsorptive removal of organics, photocatalytic oxidation resulted in a 60% lower organic concentration when activated carbon was present after the same UV irradiation time.

Keywords: activated carbon; greywater; hybrid process; photocatalytic oxidation; synergy

Introduction

Because of its segregation from toilet and industrial wastewaters, greywater is a better source for reuse than municipal effluents, as it contains lower concentrations of nutrients, faecal pathogens and hazardous industrial chemicals. Biological treatment, even in low technological processes such as intermittently fed subsurface vertical-flow constructed wetlands, yields effluents with concentration of total organic carbon (TOC) within the range 5–15 $mg\,L^{-1}$ [1]. In another study [2], greywater was collected from bathroom sinks, baths and showers and treated in a subsurface horizontal flow reed bed. The chemical oxygen demand (COD) of the effluent was 17 $mg\,L^{-1}$, which can be assumed to be equivalent to a TOC concentration of about 5 $mg\,L^{-1}$. For high-quality demand reuse purposes such as groundwater recharge, TOC concentrations have to be reduced to lower concentrations (0.5–2 $mg\,L^{-1}$), depending on legal regulations. Also, organic micropollutants found in biologically treated greywater [3] must be removed. A sustainable way of achieving these goals is the advanced oxidation process of solar heterogeneous photocatalytic oxidation (PCO), the illumination by sunlight of semiconductor particles suspended in the wastewater.

However, little information is available on the space demand for solar wastewater treatment by heterogeneous PCO. In a recent study [4], areas required in a sunny region for solar PCO of different pretreated wastewaters were estimated on the basis of UV dose-derived rate constants obtained in laboratory-scale experiments for the following conditions: 2 $g\,L^{-1}$ TiO_2 P25 photocatalyst, insolation of 3.9 $kWh\,m^{-2}\,d^{-1}$ (a 5% proportion of this being assumed to be represented by UV photons [5]), and TOC reduction to 2 $mg\,L^{-1}$ (or COD reduction to 5 $mg\,L^{-1}$) within one day. Area demands were in the range 20 to 1000 $m^2\,m^{-3}$ of treated wastewater. For biologically pretreated greywater the specific area demand was 350 m^{-1}. Braham and Harris [6] have commented on these results that solar PCO is unsuitable for the treatment of large volumes.

Strategies are therefore needed for making solar PCO more efficient. A very promising technique is the combination of PCO with activated carbon adsorption. It has been shown that the presence of particular activated carbon types leads to increased PCO rate

*Corresponding author. Email: holli@tuhh.de

constants for model wastewaters containing phenol [7–9], 4-chlorophenol [8,10,11], caffeic acid [12], 2,4-dichlorophenoxyacetic acid [8], the azo dye Direct Blue 53 [13], clofibric acid [14], or the antineoplastic cytarabine [15].

The synergy observed in the PCO/activated carbon combination process is usually quantified in terms of the synergy factor (SF), the ratio of the PCO rate constant in the presence (k_{PCO_AC}) and the absence (k_{PCO}) of activated carbon [8–10]:

$$SF = k_{PCO\_AC}/k_{PCO} \quad (1)$$

One reason for the synergy is the short diffusion pathways for organic molecules from the adsorbent to the photocatalyst particles which are directly adhered to the activated carbon [16]. Accordingly, SFs for the PCO/activated carbon hybrid process have been found to be related to the interfacial areas between activated carbon and photocatalyst particles [8]; the synergy increases with increasing interface contact between TiO_2 and activated carbon. However, when the contact area exceeds 50% of the total surface of the photocatalyst the synergetic effect decreases [11].

Additionally, particular functional groups (e.g. carboxylic acid or cyclic ether groups) on activated carbon microcrystallite surfaces are hypothesized to interact coordinatively with Ti centres located on TiO_2 surfaces [17], especially in the anatase form, which is the predominant TiO_2 modification present in P25. Anatase shows a higher oxygen vacancy (i.e. a deficiency in oxygen ligands) of Ti atoms on its surface than does rutile [18]. Coordination of Ti centres with oxygen-containing activated carbon-functional surface groups enables the transfer of electrons between photocatalyst and adsorbent [17,19]. Cordero *et al.* [20] assumed that photo-induced mobile electrons in the photocatalyst can be transferred to the neighbouring activated carbon surface in this way. Thus, the recombination of photo-induced electrons and holes within the photocatalyst is diminished, leading to a prolonged lifetime of the holes and a higher probability of their arrival at the photocatalyst surface and consequently to a more efficient oxidation of organics in the vicinity of the photocatalyst [16]. The surface chemistry (and therefore the source material and the activation process) of the activated carbon affects both the photocatalyst/activated carbon interfacial area and the charge (electron or hole) transfer between the two solids [20]. Therefore, only particular activated carbons cause synergetic effects in the PCO/activated carbon combination process.

From PCO experiments in the presence of sawdust-derived carbons activated under different conditions, there is evidence that the structure of graphene layers in activated carbon microcrystallites also influences the extent of synergy in photocatalytic TiO_2/activated carbon systems [11]; the lower the disorder of the graphene layers (i.e. the closer is their structure to pure graphite), the higher the electrical conductivity of the activated carbon. When electron semiconductivity of the graphitic microcrystallites in the activated carbon is sufficient, the activated carbon is able to transport charge carriers injected from contacting photo-excited TiO_2 particles. This supports the effect mentioned above of hole–electron recombination suppression within the photocatalyst when particular activated carbon types are added to the PCO process. Overall, the impact of activated carbon properties on synergy between PCO and activated carbon adsorption is very complex.

In order to investigate whether synergy can also be observed by combining PCO with activated carbon adsorption with wastewaters in practice, biologically pretreated greywater was concentrated by vacuum evaporation and subjected to PCO in the absence and the presence of an activated carbon type for which synergy had been demonstrated in previous studies. Non-enriched pretreated greywater would not have allowed the kinetics to be recorded, as its TOC is very low and activated carbon adsorption might result in TOC concentrations close to limits of detection, yielding unreliable results. Additionally, a polar non-aromatic compound, tetraethylene glycol dimethyl ether (TetraEGDME; 2,5,8,11,14-pentaoxapentadecane), which is nonionic but nonetheless water-soluble due to its polarity, was tested for eventual synergy in the combination process PCO/activated carbon. TetraEGDME has been detected in municipal effluents in the $\mu g\,L^{-1}$ range [21,22], and also in runoff from fields irrigated with treated wastewater [23] as well as in wastewaters of two different waste oil refineries [24,25]. The experiments with greywater concentrate and TetraEGDME model wastewater were compared by means of synergy studies with phenol.

Materials and methods

Materials

Two types of powdered activated carbon (PAC) were investigated; the first (analytical grade, article 102186) was purchased from Merck Eurolab (Darmstadt, Germany), and the other (Hydraffin WG, for water and wastewater treatment) from Lurgi (Frankfurt am Main, Germany). Properties of the carbons are summarized in Table 1. Titanium dioxide (Aeroxide P25) was provided by Evonik Industries AG (Hanau–Wolfgang, Germany), TetraEGDME (synthesis grade, purity >98%) and phenol (analytical grade) by Merck Eurolab. A grab sample of biologically pretreated greywater was taken from the effluent of a subsurface vertical-flow constructed wetland, with intermittent feeding of greywater separately collected in the eco-settlement Lübeck–Flintenbreite. Operation of the constructed wetland is described elsewhere in greater detail [3]. The non-purgeable TOC (np-TOC) concentration of the clear constructed wetland effluent was $7.0 \pm 0.2\,mg\,L^{-1}$, and total inorganic carbon (TIC) concentration was $78.5 \pm 2\,mg\,L^{-1}$.

Table 1. Properties of activated carbons investigated; information by suppliers unless otherwise stated.

	Merck 102186	Hydraffin WG
Water content (%)	<10	<10
Ash content (%)	<1	about 5
pH (in deionized water)	4–7	3–5
BET surface ($m^2\,g^{-1}$)	775[a]	1100
Particle size	about 60 μm[a], 50% ≤ 30 μm, 90% ≤ 100 μm	85% ≤ 40 μm
Iodine uptake ($mg\,g^{-1}$)	888	1050

[a] from [7].

A second grab sample used for recording an adsorption isotherm exhibited an np-TOC of $6.1 \pm 0.2\,mg\,L^{-1}$ and a TIC of $73.1 \pm 0.4\,mg\,L^{-1}$. The np-TOC concentration of a third sample taken from the same source in order to quantify different classes of organic compounds by liquid chromatography coupled with organic carbon detection was $6\,mg\,L^{-1}$.

Concentration of biologically treated greywater by vacuum evaporation

The effluent of the constructed wetland was subjected to vacuum evaporation in a rotary evaporator at 80°C. After evaporating 20 L to a final volume of 2 L, the concentrate was re-diluted with 2 L of original biologically pretreated greywater in order to obtain sufficient fivefold concentrate for PCO experiments in duplicate.

UV irradiation experiments

The following samples were subjected to UV irradiation at ambient temperature in 1 L batches:

- 1 mM phenol ($94\,mg\,L^{-1}$) solution in deionized water or tap water,
- 0.225 mM TetraEGDME ($50\,mg\,L^{-1}$) solution in deionized water or tap water, and
- a fivefold concentrate of biologically pretreated greywater.

The pH of the model wastewaters and the greywater concentrate was not further adjusted but was recorded during UV irradiation. Solutions were placed in slim 2 L beakers (inner diameter 10.8 cm) which were stirred by means of 7 cm magnetic stirring bars at a speed of $300\,min^{-1}$ (Figure 1). Prior to UV irradiation the suspensions were stirred for 1 h in the dark, according to [7]. UV irradiation was performed with face tanners (HD 172, Philips, Hamburg, Germany) placed 20 cm above the liquid surface. UV intensity was measured using a pyranometer (CMP 3, Kipp & Zonen, Delft, Netherlands) and was $15\,W\,m^{-2}$ at the liquid surface. The face tanners exhibited an emission maximum

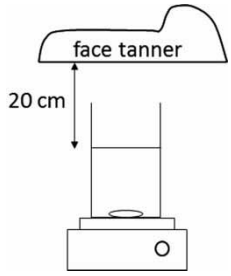

Figure 1. Experimental setup for photolysis, PCO and PCO/PAC experiments.

at 352 nm. Although not thermostated, the temperature of the reactor contents was sufficiently constant at 27 ± 2°C, slightly above room temperature due to heat emission from the UV lamps. Different kinds of irradiation experiments were performed, including photolysis (without addition of TiO_2 and PAC), PCO (with addition of $2.5\,g\,L^{-1}$ TiO_2 P25), and PCO in the presence of PAC (with addition of $2.5\,g\,L^{-1}$ TiO_2 P25 and $0.5\,g\,L^{-1}$ of one of the two investigated activated carbon types).

Samples (50 mL) were taken from the stirred reactors at different times. Water evaporating from the reactors was replenished with deionized water prior to sampling. All samples were membrane-filtered (Magna Nylon filters, pore width 0.45 μm, Carl Roth GmbH, Karlsruhe, Germany) prior to DOC, DIC and phenol analysis. Some experiments were performed in multiplicate as indicated in the results and discussion section. Apparent first-order rate constants, k, were derived from the slopes of the regression lines recorded for the different experiments:

$$\ln(c_0/c) = kt, \tag{2}$$

where c is concentration of phenol, DOC or np-DOC, c_0 the respective concentration at the beginning of UV irradiation and t is the irradiation time. As the reaction rate depends on temporary organic concentrations, and concentration of the organics was increasing due to water loss by evaporation during UV irradiation, Equation (2) is a simplification. However, as enrichment factors due to water evaporation between two sampling events were less than 1.1, this simplification was regarded as tolerable.

Adsorption kinetics in the dark

1 L suspensions of $0.5\,g\,L^{-1}$ PAC in solutions of phenol ($94\,mg\,L^{-1}$) or TetraEGDME ($50\,mg\,L^{-1}$) were magnetically stirred in closed bottles in a thermostated water bath to maitain the temperature at 27°C for up to 48 h. Light was excluded from the bottles by wrapping them in aluminium foil. At different time intervals, 30 mL samples were pipetted from the stirred solutions and filtered over a folded paper filter. Filtrates of phenol solutions were subjected to photometric phenol analysis, while the TetraEGDME solution filtrates were analysed for TOC.

Table 2. Ranges of pH and DO in the different reaction mixtures during UV irradiation.

Experiments	Matrix	pH	DO [mg L^{-1}]	*n* (number of experiments)
Phenol photolysis	DI	5.2–7.0	5.5–6.9	8
Phenol PCO	DI	3.9–4.8	5.7–6.9	5
Phenol PCO + Merck AC	DI	4.2–5.3	5.3–6.7	4
Phenol PCO + Hydr. WG AC	DI	3.4–4.1	n.a.	1
Phenol PCO	TW	7.6–8.4	n.a.	1
Phenol PCO + Merck AC	TW	7.7–8.3	n.a.	1
TetraEGDME PCO	TW	8.0–8.4	n.a.	1
TetraEGDME PCO + Merck AC	TW	8.0–8.4	n.a.	1
TetraEGDME PCO	DI	3.4–5.5	n.a.	1
TetraEGDME PCO + Merck AC	DI	3.4–5.2	n.a.	1
GW conc. PCO	36 mmol L^{-1} HCO_3^-	8.2–9.1	n.a.	2
GW conc. PCO + Merck AC	36 mmol L^{-1} HCO_3^-	8.4–9.2	n.a.	2

n.a.: not analyzed; DI: deionized water; TW: tap water; GW conc.: greywater concentrate.

Greywater adsorption isotherm

Different masses of the Merck PAC were suspended in 50 mL portions of non-concentrated biologically pretreated greywater, giving PAC concentrations between 0.1 and 20 g L^{-1}. These suspensions were agitated for 5 days at 21°C on a mechanical shaker at 150 min^{-1}. Subsequently the PAC was allowed to settle and the supernatant liquor was filtered over 0.45 μm porosity membrane filters. Filtrates were analyzed for np-DOC.

Analyses

Phenol concentrations were analyzed photometrically by recording the absorbance of membrane-filtered samples in quartz glass cuvettes between 200 and 400 nm using a double-beam photometer (V–550, Jasco, Gross-Umstadt, Germany). The height of the absorption maximum at 270 nm was corrected by subtracting the height of the baseline drawn between the two valleys neighbouring the maximum. The baseline-corrected absorbances were calibrated against phenol solutions of known concentration.

DOC concentrations of phenol and TetraEGDME solutions were measured using the difference method. Due to the high TIC concentrations, greywater samples were analyzed for np-DOC. Both analytical procedures were completed in accordance with German standard methods [26] using a TOC analyser multi-N/C 3000 (analytikJena AG, Jena, Germany) under the following conditions: furnace temperature, 850°C; catalyst, CeO_2; incineration gas, CO_2-free air. For np-DOC analysis, samples were acidified to pH 1–2 with concentrated HCl and purged 20 min with CO_2-free air prior to DOC analysis. TIC and DIC were analyzed in the same analyzer following the difference method.

Different classes of organic greywater constituents (polysaccharides, humic substances, building blocks, low molecular weight organic acids) in constructed wetland effluent samples were analyzed subsequent to membrane filtration (0.45 μm pore width). Liquid chromatography was employed, with organic carbon detection (LC–OCD; DOC–Labor Dr. Huber, Karlsruhe, Germany) as described in [27] using a size exclusion column HW–55S and FIFFIKUS software for quantification. The LC–OCD analyzer was equipped with a 190 nm irradiation thin-film reactor organic carbon detector and a UV detector.

Dissolved oxygen concentration and pH in the reactors were determined using the respective probes (WTW, Weilheim, Germany).

Results and discussion

Matrix properties

Table 2 shows the range of pH and dissolved oxygen concentration established in the different reaction mixtures during UV irradiation. Dissolved oxygen concentration was only recorded for phenol degradation in a deionized water matrix (six experiments on photolysis, two experiments on PCO and four experiments on the combination of PCO with Merck PAC addition). It was clearly demonstrated that stirring of the reaction mixtures supplied sufficient dissolved oxygen (6 to 7 mg L^{-1}).

Comparison of the pH of phenol solutions in deionized water during photolysis to pH of phenol/TiO_2 suspensions in deionized water during PCO shows that TiO_2 addition decreased the pH due to its acidic $\equiv TiOH_2^+$ surface functional groups. Addition of Merck PAC slightly raised the pH, while addition of Hydraffin WG PAC decreased the pH by about 0.5 units. This is in accordance with the more acidic character of Hydraffin WG (Table 1). The matrices of the solutions investigated largely influenced pH; while TiO_2 suspensions in phenol solutions with deionized water caused pH between 3.9 and 4.8, the same suspensions in a tap water matrix exhibited a pH range of 7.6 to 8.4 due to the dissolved hydrogen carbonate in tap water (TIC concentration 21.6 mg L^{-1}). A similar pH increase was observed when deionized water was replaced by normal tap water with TetraEGDME as the solute. The highest pH was found in TiO_2 suspensions in concentrated biologically

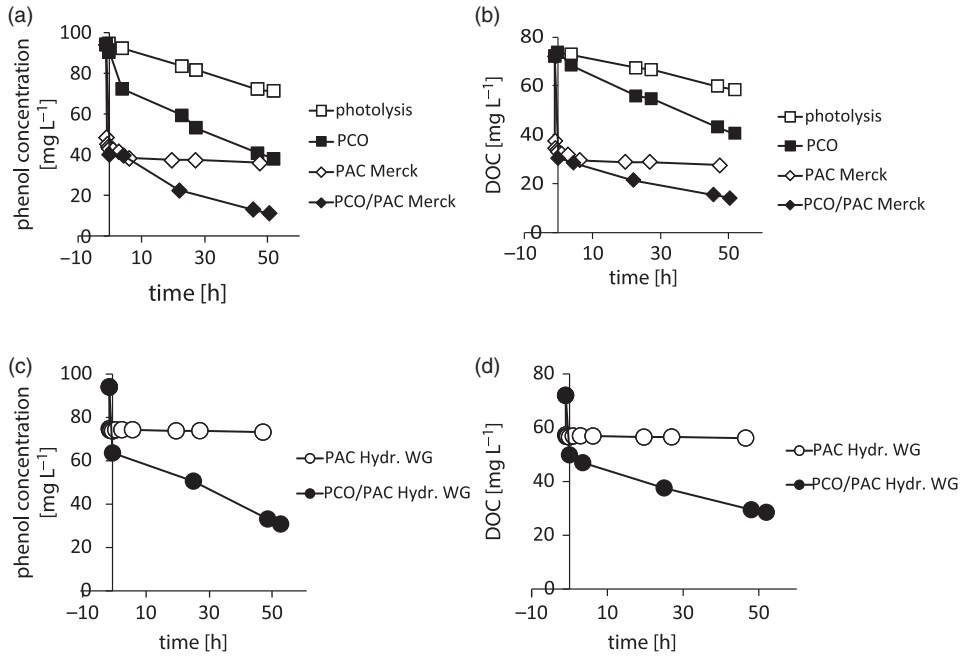

Figure 2. Kinetics for phenol removal by photolysis, PCO, adsorption to Merck PAC and PCO in the presence of Merck PAC in terms of (a) phenol and (b) DOC concentrations, and phenol removal by adsorption to Hydraffin WG PAC and PCO in the presence of Hydraffin WG PAC in terms of (c) phenol and (d) DOC concentration.

pretreated greywater, which showed a TIC concentration of 432 mg L^{-1}. While the pH at the start of the experiment was 8.2 to 8.4, it increased to above 9 during PCO, irrespective of the presence of PAC.

Reference experiments with phenol solutions and the impact of activated carbon type

The results of photometric phenol analysis might be slightly affected by aromatic phenol PCO intermediates (1,2-dihydroxybenzene and 1,4-dihydroxybenzene as predominant intermediates, and 1,2,3-trihydoxybenzene, 1,2,4-trihydroxybenzene [28], and benzoquinone [29] as minor products). Most of these substances exhibit absorption maxima sufficiently remote from the 270 nm absorption maximum of phenol, and the valley-to-valley maximum baseline subtraction prevents overestimation of phenol concentration. Only 1,2-dihydroxybenzene (maximum at 277 nm) might interfere, since it shows a shoulder on the phenol maximum. However, valley-to-valley correction minimized this interference.

It was intended to determine whether the PAC-derived synergy for phenol PCO observed in other studies [7,8] could be reproduced in a reactor system with lower UV intensity, different UV emission spectrum and different reactor geometry at higher temperatures. The experiments of Matos *et al.* [7,8] were therefore repeated with a modified experimental setup, as described in the methodology section, but with the same type of photocatalyst and PAC and similar concentrations of phenol, photocatalyst and PAC. All the results given in Figure 2 are displayed at a starting time of −1 h. The period between −1 h and 0 represents the stirring phase in the dark prior to each UV irradiation experiment. UV irradiation was started at time 0. Analogously, the first hour of the adsorption experiment in the dark is displayed in the time interval between −1 h and 0. The graphs shown in the upper part of Figure 2 represent (a) the kinetics for phenol removal, and (b) for DOC removal, during photolysis (UV irradiation without photocatalyst and PAC), PCO without PAC, and phenol adsorption by Merck PAC and PCO in the presence of the Merck PAC. Figure 2(c) shows phenol concentrations during phenol adsorption by Hydraffin WG and during phenol PCO in the presence of this PAC. Figure 2(d) presents the DOC concentrations obtained in the same experiments.

In contrast to the results of Matos *et al.* [7,8], photolysis of phenol was more pronounced in the present study, probably explained by the different types of UV lamp employed. Matos *et al.* [7,8] used a high-pressure mercury lamp giving an emission spectrum with predominant intensities at 365 and 366 nm, whereas the face tanner used in the present study was characterized by a broad emission range between 320 and 420 nm with a maximum at 352 nm, which might cover a part of the absorption maxima of phenol and its photolysis intermediates. The broad UV emission maximum of the face tanner reproduces more realistically the sky and solar radiation in the UV range than the UV line spectra of a high-pressure mercury lamp.

The equilibrium of phenol adsorption to Merck PAC in the absence of TiO_2 and UV irradiation was not completely reached within the first hour of stirring at 27°C

(Figure 2(a) and (b)). This is in contrast to phenol adsorption on the same activated carbon, but at 20°C [7], when at 20°C equilibrium was reached after 15 min. The anomaly is explained by slower mass transfer at a higher temperature due to a smaller driving force, which was evidently not compensated by an increase in the mass transfer coefficient with increasing temperature. However, the major part of the phenol was adsorbed within the first hour of stirring, as the phenol concentration decreased from 94 to 42.3 mg L^{-1}, equivalent to a reduction in DOC concentration from 72 to 34.2 mg L^{-1} (Figure 2(b)). During the following 6 h the phenol concentration was reduced by 4.6 mg L^{-1} and in the final 41 h by a further 2.5 mg L^{-1}. Although some phenol removal was detectable in the phase after the first hour of stirring, this does not require correction of the data collected for phenol PCO in the presence of Merck PAC, since the decrease of phenol concentration in the second phase was small compared to the phenol removal by combining PCO with Merck PAC (open and closed diamonds in Figure 2(a)). While after 47 h stirring in the dark 17% of the phenol concentration present at $t = 0$ (at the end of the first hour equilibration period) was removed from the liquid phase by further adsorption by Merck PAC, almost 70% of the phenol was removed by the PCO/Merck PAC hybrid process over the same time. In contrast to Merck PAC, the Hydraffin WG PAC reached the adsorption equilibrium at 27°C after only 1 min (Figure 2(c) and (d)). However, the equilibrium phenol concentration in the aqueous phase was much higher (74 mg L^{-1}) than with Merck PAC. The adsorbability of phenol on both PAC types showed the opposite trend to the BET surface and the iodine number (Table 1). On the other hand, this result is in accordance with recent findings indicating that phenol is adsorbed to a greater extent by activated carbons with a lower ash content [30]; the Merck PAC contained less than 1% ash, while the ash content of the Hydraffin WG PAC was about 5% (Table 1).

Figure 3 illustrates the rate constants (based either on phenol concentrations or on DOC) for all the UV irradiation experiments and the adsorption in the dark for phenol solutions in deionized water. By analogy with the PCO experiments, in which the first hour without UV irradiation was used to establish the adsorption equilibrium as completely as possible, the liquid phase phenol concentrations which were recorded in the first hour during adsorption by the two activated carbons in the dark were not considered for calculating rate constants. Rate constants for phenol adsorption in the dark, ignoring the first hour of stirring (0.0035 h^{-1} for Merck PAC and 0.0003 h^{-1} for Hydraffin WG PAC), were small compared to the rate constants recorded in the corresponding PCO/PAC experiments. The addition of Merck PAC increased the PCO rate constant based on phenol degradation from 0.0125 to 0.0253 h^{-1}, greater than by merely adding the adsorption rate constant to the PCO rate constant, which would result in 0.0160 h^{-1}. Even when the standard deviations for PCO and PCO/Merck PAC rate constants were added to this

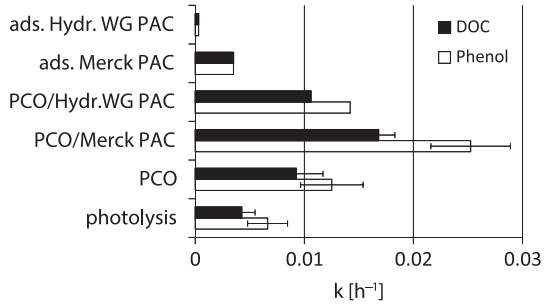

Figure 3. Apparent first-order rate constants (based on phenol concentration and on DOC) for phenol degradation by photolysis ($n = 8$), PCO ($n = 5$), and PCO in the presence of Merck PAC ($n = 4$) or Hydraffin WG PAC ($n = 1$). Matrix: deionized water.

sum, the result (0.0225 h^{-1}) was still 11% below the rate constant of the PCO/Merck PAC hybrid process. At least the synergetic trend observed in other investigations [7,8] was reproduced in these experiments.

Matos *et al.* [7] found rate constants for phenol PCO (based on phenol concentrations) of 0.336 h^{-1} (without PAC) and 0.834 h^{-1} (with Merck PAC), while the rate constants achieved in the present study were only 0.0125 ± 0.0029 h^{-1} without PAC and 0.0253 ± 0.0037 h^{-1} in the presence of Merck PAC (Figure 3). The larger rate constants obtained in [7] are clearly attributable to a stronger UV lamp (125 W power uptake) located very close to a much smaller illuminated volume (20 mL) of the phenol/TiO_2 (PAC) suspensions in comparison to the present study (75 W power uptake, 20 cm distance between lamp and suspension surface, 1000 mL suspension volume). The SF derived from phenol-based apparent first-order rate constants in the present study was 2.02 ± 0.75, while Matos *et al.* [7] found a slightly larger SF of 2.5 with the same concentrations of phenol, TiO_2 and PAC, but applying different irradiation conditions. However, the SFs obtained in both studies were not very different after allowing for the uncertainties inherent in the results presented here.

DOC removal rate constants in the PCO experiments presented were lower than the rate constants for phenol removal (Figure 3). However, the rate constant for DOC removal was also increased by adding Merck PAC to the PCO process. The sum of the DOC-based rate constants for PCO (0.0093 h^{-1}) and for adsorption on to Merck PAC (0.0037 h^{-1}), ignoring the first hour adsorption equilibration period, was definitely smaller than the rate constant of the PCO/Merck PAC hybrid process (0.0168 h^{-1}). On the other hand, when the standard deviations of PCO and PCO/Merck PAC rate constants are added, the result (0.0169 h^{-1}) is larger than the DOC-based rate constant for the PCO/Merck PAC hybrid process. This means that the synergy of Merck PAC addition to phenol photocatalysis is not completely clear once all the organics in the reaction mixture, including phenol and temporary oxidation intermediates, are considered.

The SF calculated from DOC-based rate constants was slightly lower (1.81 ± 0.64) than the SF based on phenol analysis (2.02 ± 0.75), indicating that the synergy achieved by Merck PAC addition is more marked for PCO of the mother molecule than for PCO of oxidation intermediates. According to the discussion above, it cannot be ruled out that the enhancement of DOC-based PCO rate constant by the addition of Merck PAC depends only on additional (residual) adsorption during the 50 h irradiation interval, because phenol adsorption equilibrium was not completely established within this period.

As explained in the Introduction, synergy between activated carbon adsorption and photocatalysis depends on the activated carbon being in full contact with the photocatalyst. This includes the surface functional groups responsible for interaction with the photocatalyst as well as the extent of order of graphene layers enhancing activated carbon conductivity. Accordingly, the second PAC tested (Hydraffin WG) did not cause a pronounced synergy in phenol PCO (Figure 3). The SF for Hydraffin WG PAC addition to phenol PCO was 1.13 (calculated from rate constants based on phenol concentrations). The rate constant in the presence of Hydraffin WG PAC was smaller than the sum of PCO rate constant and its standard deviation. Poor phenol adsorption to Hydraffin WG PAC is supposed to contribute to lack of synergy for this PAC type, as the synergy implies adsorption of the organics on the activated carbon. On the other hand, addition of Hydraffin WG did not impair the PCO rate constants. Therefore, even with a SF of around 1, dosing of Hydraffin WG PAC offers a benefit, inasmuch as it contributes to phenol removal from the liquid phase by adsorption additional to PCO; after 50 h, PCO alone resulted in a residual phenol concentration in the liquid phase of 38 mg L^{-1} (Figure 2(a)), while PCO in the presence of Hydraffin WG PAC led to a residual phenol concentration of only 31 mg L^{-1} (Figure 2(c)).

Impact of the type of organic compound and inorganic matrix on synergy

Results of experiments performed with 50 mg L^{-1} TetraEGDME (instead of 94 mg L^{-1} phenol) solution in deionized water are shown in Figure 4. As in Figure 2, the period from −1 h to time 0 is the 1 h stirring phase without UV irradiation. TetraEGDME photolysis was negligible in comparison to photolysis of phenol. Figure 4 shows that 68% of TetraEGDME was adsorbed at 27°C, not very different from the 62% phenol adsorption to Merck PAC at this temperature (Figure 2(a) and (b)). However, the initial TetraEGDME concentration on a mass base was only about half as large as phenol concentration before PAC addition. On a molar base, TetraEGDME concentration was even 75% lower than the phenol concentration. In contrast to phenol, TetraEGDME adsorption reached equilibrium already 30 min after adding the Merck PAC (at −0.5 h in Figure 4). Dosing of 0.5 g L^{-1} Merck PAC to PCO of the

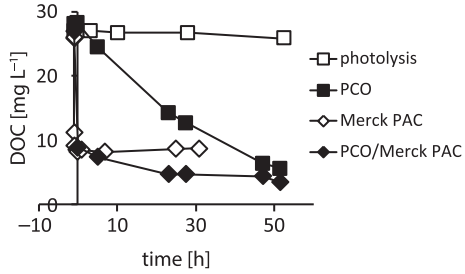

Figure 4. TetraEGDME removal by photolysis, adsorption by Merck PAC, PCO; and PCO in the presence of Merck PAC.

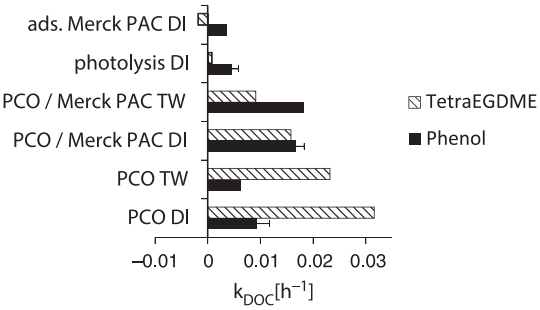

Figure 5. Apparent first-order rate constants (based on DOC) for phenol removal by adsorption in deionized water (DI), photolysis in deionized water, PCO in deionized water ($n = 4$) and in tap water (TW, $n = 1$), and by PCO in the presence of Merck PAC in deionized water ($n = 4$) and in tap water ($n = 1$). Constants from experiments with TetraEGDME are also presented (all TetraEGDME experiments: $n = 1$).

TetraEGDME solution had the advantage that DOC was rapidly diminished by more than 60% (as also shown for adsorption alone), but the PCO rate in the presence of PAC was much smaller than without PAC (Figure 4). Following a 50 h UV irradiation period in the presence of Merck PAC, the DOC was not markedly lower than in the absence of PAC. This contrasts with the results obtained with phenol solutions in deionized water (compare Figure 2(b)).

In Figure 5 the DOC-based apparent first-order rate constants for photolysis, adsorption on Merck PAC, PCO with and without Merck PAC of phenol and TetraEGDME solutions in deionized water are compared. Rate constants from PCO and PCO/Merck PAC experiments but with tap water as the matrix are also shown. TetraEGDME was removed by PCO in the absence of PAC with a more than threefold greater rate constant compared to phenol, irrespective of the matrix. In tap water, the DOC-based PCO rate constant was 29% lower for phenol and 26% lower for TetraEGDME than in deionized water. This can be explained by the presence of the radical scavenger HCO_3^- in tap water (tap water TIC concentration: 21.6 mg L^{-1}, which is equivalent to 1.8 mmol L^{-1} hydrogen carbonate ion).

PAC addition obviously prevented phenol PCO from inhibition by the radical scavenger hydrogen carbonate, as indicated by similar rate constants for the PCO/PAC hybrid process for phenol in deionized and tap water. A possible

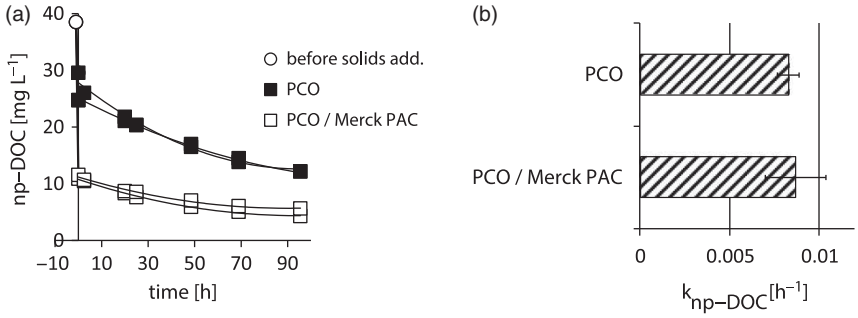

Figure 6. (a) Kinetics of np-DOC removal from biologically pretreated greywater concentrate by PCO and by PCO in the presence of Merck PAC, and (b) the related apparent first-order rate constants from experiments performed in duplicate.

explanation may be that hydroxyl radicals do not play a predominant role in the hybrid process for organics when the SF is above 1. Hypothetically, aromatic molecules (such as phenol) adsorbed on the inner activated carbon surface by charge-transfer interactions, e.g. with quinone-like PAC surface functional groups or with graphene layers, might be oxidized directly by electron holes injected from an illuminated attached TiO_2 particle into the PAC grain and transferred via well-ordered graphene layers to the adsorption site. Thus, hydroxyl radicals may not be necessary for phenol oxidation in the PCO/PAC hybrid process when the PAC has been properly selected.

Baransi *et al.* [12] have discussed π–π interactions of phenolic compounds with graphene layers of activated carbon and that these might lead to an increased photocatalytic degradation in the photocatalyst/activated carbon/UV system, even when these organic compounds are not in direct contact with the photocatalyst but are adsorbed within the inner pores of the activated carbon particle to which a hole has been injected by an adjacent illuminated photocatalyst particle. This assumption is based on the observation that nearly 90% of polyphenols were removed from an anaerobically pretreated olive mill wastewater by the PCO/PAC hybrid process, while COD was only eliminated by less than 60%, indicating that the adsorbable polyphenols were removed by the hybrid process to a greater extent than the other organic constituents of this wastewater. With TetraEGDME, PAC addition did not protect from hydroxyl scavenging by hydrogen carbonate. This can be concluded from the much lower PCO/Merck PAC hybrid process rate constant in the tap water matrix (0.0091 h^{-1}) than in deionized water (0.0158 h^{-1}), as shown in Figure 5.

Of course, PCO rate constants in the tap water matrix might be affected not only by the radical scavenger hydrogen carbonate but also by pH. The pH of the TiO_2 suspensions in the tap water matrix was around 8, while pH of TiO_2 suspensions in deionized water was between 3.4 and 5.5 (Table 2). It is assumed that phenol as well as carboxylic acid oxidation intermediates of both model compounds (phenol and TetraEGDME) are adsorbed more efficiently to the photocatalyst at lower pH and are thus more efficiently oxidized; at pH > point of zero charge (PZC), the TiO_2 photocatalyst exhibits negative surface charges, repelling phenolate and carboxylic acid anions which are predominantly negatively charged when the pH exceeds the pK_a of the respective compounds. Obviously, this inhibition by pH was not particularly pronounced for phenol, because the pKa of phenol is 9.98 [31].

The most striking finding shown in Figure 5 is the antagonistic action of PAC addition on PCO of TetraEGDME. While DOC-based SFs achieved by Merck PAC addition to phenol PCO were 1.81 $\pm$ 0.64 in deionized water, and even 2.95 in tap water, the respective factors for DOC removal from TetraEGDME solutions were 0.5 in deionized water and as low as 0.39 in tap water. This clearly shows an inhibition of photocatalytic TetraEGDME removal when the Merck PAC was added. Inhibition was obviously a consequence of additional photocatalyst shading by PAC particles in the suspension. The inhibitory effect of photocatalyst shading by PAC particles was probably more than compensated by synergy in case of phenol and Merck PAC. It can be assumed that there was even a small degree of compensation of the shading effect by synergy in case of phenol and the Hydraffin WG PAC, because according to Figure 3 the SF here was around 1 (no inhibition).

A general conclusion to be drawn from the experiments is that aliphatic organic compounds such as TetraEGDME are not susceptible to the synergetic effect delivered by Merck PAC addition to PCO. Accordingly, synergy was so far observed exclusively for aromatic compounds [7–15]. Since charge carriers injected into activated carbon particles by illuminated TiO_2 particles can migrate through the activated carbon, oxidative reactions initialized by holes are assumed to take place also on the activated carbon surface in the PCO/activated carbon process via activated carbon functional groups/aromatic adsorbate π–π interactions, as explained above. This assumption has been corroborated by the recent finding that special types of activated carbon themselves, i.e. in the absence of known photocatalysts such as TiO_2, are able to catalyze phenol photodegradation [32,33].

Experiments with greywater concentrate

Figure 6(a) shows np-DOC removal kinetics for the fivefold concentrate of biologically pretreated greywater. Although

the np-DOC removal rate in the presence of Merck PAC was lower than without PAC, due to a lower dissolved organic concentration, the PCO rate constant was not markedly affected by PAC addition for greywater organics (Figure 6(b)); the SF was 1.07 ± 0.26. This is different from the synergy obtained with phenol. On the other hand, PAC addition did not lead to impairment of greywater concentrate PCO efficiency, in contrast to findings with TetraEGDME. Also in the case of greywater, a SF of around 1 is beneficial for the hybrid process as activated carbon removes additional DOC by adsorption. Accordingly, a recent study [34] has indicated that addition of $1\,g\,L^{-1}$ Hydraffin WG PAC to PCO of biologically pretreated greywater leads to more efficient np-DOC elimination than PCO alone, even when the PAC/TiO_2 mixture has been reused 10 times. From these data it was estimated that the insolation area for solar PCO of biologically treated greywater can be reduced by a factor of 7 to achieve the same purification result when $1\,g\,L^{-1}$ Hydraffin WG PAC has been added. Efficient regeneration by UV irradiation has also been demonstrated for a TiO_2/activated carbon composite used for removal of coloured substances from secondary municipal effluent [35].

Moreover, it is noteworthy that the apparent rate constant for photocatalytic removal of np-DOC from greywater concentrate ($0.0083\,h^{-1}$) was nearly as high as that for DOC removal from phenol solutions in deionized water in the absence of PAC ($0.0093\,h^{-1}$; Figure 3) and markedly higher than for DOC removal from the phenol solution in tap water ($0.0062\,h^{-1}$; Figure 5). This was not expected, since there was a high concentration of the radical scavenger hydrogen carbonate in the greywater concentrate; TIC was $432\,mg\,L^{-1}$ which is equivalent to $36\,mmol\,L^{-1}$ hydrogen carbonate. On the other hand, the TiO_2/DOC mass ratio in the PCO experiments with greywater concentrate was more than twice as high as during photocatalytic phenol degradation. It cannot be excluded that the catalyst/organics mass ratio also influences the SF.

A great many of the organic constituents of biologically treated greywater are represented by humic substances [36]. In another effluent sample of the same constructed wetland for greywater treatment, the following groups of organics were quantified by LC–OCD analysis: polysaccharides ($100\,\mu g\,DOC\,L^{-1}$), humic substances ($3530\,\mu g\,DOC\,L^{-1}$), building blocks ($880\,\mu g\,DOC\,L^{-1}$), and low molecular weight organic acids ($790\,\mu g\,DOC\,L^{-1}$). Humic substances contain aromatic structures. Therefore, the absence of synergy for biologically treated greywater was not expected. On the other hand, no synergy in humic acid PCO (using TiO_2 prepared by the sol–gel method) was detected when adding a nut kernel-derived activated carbon (70–100 mesh) [37]. It cannot be excluded that the reason for the absence of synergy in that study was an activated carbon type not exhibiting the properties required for synergy, as discussed above (particular oxygen-containing functional surface groups, undisturbed graphene layers, sufficiently large contact interface between activated carbon and photocatalyst). However, the rate constant for photocatalytic humic acid mineralization was increased when the same activated carbon was coated with TiO_2 by a sol–dipping–gel method [37]. Therefore, TiO_2-coated activated carbon seems to have advantages over simple mixtures of activated carbon and photocatalyst. A disadvantage of composite catalysts is that they are not common industrial products and have to be specially synthesized, involving additional know-how and expense.

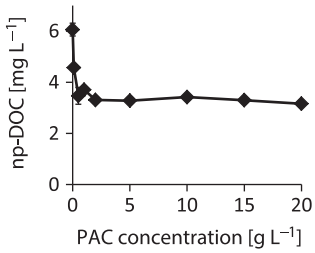

Figure 7. Concentrations of residual np-DOC in biologically pretreated greywater after 5 days shaking with different concentrations of Merck PAC.

Another reason for the absence of synergy in the PCO/Merck PAC hybrid process treating the greywater concentrate might be the size of a particular fraction of the organic molecules contained in greywater. Figure 7 shows an adsorption isotherm for the Merck PAC recorded with another sample of biologically pretreated greywater, which was not however concentrated by evaporation. In order to ensure complete establishment of adsorption equilibrium, a very long agitation time of five days was selected. Once the PAC concentration exceeded $2\,g\,L^{-1}$, no further np-DOC reduction was observed with increasing PAC concentration.

This means that there is a residual organic concentration in the biologically treated greywater which is not adsorbable by the Merck PAC. The non-adsorbable concentration is about 3.3 mg np-DOC L^{-1} or 54% of the original np-DOC of the non-concentrated biologically pretreated greywater. It can be seen that this percentage was lower for the greywater concentrate (41%) when comparing np-DOC at the start of the PCO experiment (i.e. subsequent to the 1 h stirring period in the dark) without PAC addition and at $t = 0$ of the hybrid process PCO/Merck PAC (Figure 6(a)). It has to be considered that these np-DOC concentrations at irradiation time zero were also affected by adsorption on the photocatalyst.

The organic molecules representing the non-adsorbable residue (among them humic substances formed during biological greywater treatment) are simply too large to enter the pores inside the activated carbon particles. Of course, these non-adsorbed substances would be excluded from being oxidized by holes injected from illuminated TiO_2 particles into the activated carbon as discussed above. Therefore, very large humic matter molecules are not susceptible to the synergetic effect provoked by addition of the Merck

PAC. The consequence of the lack of adsorbability of a considerable percentage of organics contained in biologically treated greywater is that separation of adsorption and subsequent off-line regeneration of the loaded adsorbent by (solar) photocatalytic oxidation in two stages as suggested in [38] is not feasible. Therefore, the advantage of separated adsorption and regeneration stages, which would allow for decoupling the mass flow of organic constituents from the volume flow of the water, cannot be utilized, at least in the case of biologically pretreated greywater. As Figure 6(a) indicates, simultaneous PCO and PAC adsorption (with at least partial *in situ* regeneration, (as demonstrated in [34] for a different PAC type) is advantageous because the hybrid process achieves lower np-DOC concentrations than each of the individual processes alone.

Conclusions

Addition of a particular activated carbon (Merck PAC) resulted in increased rate constants of TiO_2-based phenol PCO. Thus, experiments previously described in the literature could be reproduced in spite of using a different type of UV lamp and other slightly different experimental conditions. A different PAC (Hydraffin WG) did not yield any synergy in phenol PCO, confirming that only activated carbons with specific properties are able to increase PCO rate constants. PCO of the aliphatic compound TetraEGDME was even inhibited by the addition of Merck PAC, evidently due to photocatalyst shading by PAC particles. When synergy was detected, it was probably compensating for inhibitory shading effects. It is hypothesized that synergy with PAC addition only occurs in PCO of aromatic compounds. Their π–π interaction with graphene layers or particular functional surface groups within the activated carbon grain can be assumed to be a prerequisite for the synergy.

PCO of a fivefold concentrated biologically pretreated greywater was neither inhibited nor enhanced by Merck PAC addition. The synergy expected from humic substances (which also contain aromatic structures) being present in this wastewater was probably prevented because a high proportion of the greywater organics were not adsorbable on to the activated carbon. Nevertheless, addition of activated carbon to PCO of biologically pretreated greywater can be regarded as beneficial inasmuch as the adsorptive removal of organics adds to removal by photocatalytic mineralization. The results emphasize that it is important to study synergy using actual wastewaters, rather than pure aqueous solutions of model organics such as phenol.

References

[1] Z. Li, H. Gulyas, M. Jahn, D.R. Gajurel, and R. Otterpohl, *Greywater treatment by constructed wetlands in combination with TiO_2-based photocatalytic oxidation for suburban and rural areas without sewer system*, Water Sci. Technol. 48(11–12) (2004), pp. 101–106.

[2] G.P. Winward, L.M. Avery, T. Stephenson, and B. Jefferson, *Ultraviolet (UV) disinfection of grey water: Particle size effects*, Environ. Technol. 29 (2008), pp. 235–244.

[3] H. Gulyas, M. Reich, and R. Otterpohl, *Organic micropollutants in raw and treated greywater: A preliminary investigation*, Urban Water J. 8 (2011), pp. 29–39.

[4] H. Gulyas, H.B. Jain, A.L. Susanto, M. Malekpur, K. Harasiuk, I. Krawczyk, P. Choromanski, and M. Furmanska, *Solar photocatalytic oxidation of pretreated wastewaters: Laboratory scale generation of design data for technical-scale double-skin sheet reactors*, Environ. Technol. 26 (2005), pp. 501–514.

[5] B.L. Diffey, *Sources and measurement of ultraviolet radiation,* Methods (Amsterdam, Neth.) 28 (2002), pp. 4–13.

[6] R.J. Braham and A.T. Harris, *Review of major design and scale-up considerations for solar photocatalytic reactors*, Ind. Eng. Chem. Res. 48 (2009), pp. 8890–8905.

[7] J. Matos, J. Laine, and J.-M. Herrmann, *Synergy effect in the photocatalytic degradation of phenol on a suspended mixture of titania and activated carbon*, Appl. Catal., B 18 (1998), pp. 281–291.

[8] J. Matos, J. Laine, and J.-M. Herrmann, *Effect of the type of activated carbons on the photocatalytic degradation of aqueous organic pollutants by UV-irradiated titania*, J. Catal. 200 (2001), pp. 10–20.

[9] J. Xu, *Synergy effect on a suspended mixture of ceria and activated carbon for the photocatalytic degradation of phenol*, Powder Technol. 210 (2011), pp. 1–5.

[10] J.-M. Herrmann, J. Matos, J. Disdier, C. Guillard, J. Laine, S. Malato, and J. Blanco, *Solar photocatalytic degradation of 4-chlorophenol using the synergistic effect between titania and activated carbon in aqueous suspension*, Catal. Today 54 (1999), pp. 255–265.

[11] J. Matos, J.-M. Chovelon, T. Cordero, and C. Ferronato, *Influence of surface properties of activated carbon on photocatalytic activity of TiO_2 in 4-chlorophenol degradation*, The Open Environmental Engineering Journal 2 (2009), pp. 21–29.

[12] K. Baransi, Y. Dubowski, and I. Sabbah, *Synergetic effect between photocatalytic degradation and adsorption processes on the removal of phenolic compounds from olive mill wastewater*, Water Res. 46 (2012), pp. 789–798.

[13] N. Sobana and M. Swaminathan, *Combination effect of ZnO and activated carbon for solar assisted photocatalytic degradation of Direct Blue 53*, Sol. Energy Mater. Sol. Cells 91 (2007), pp. 727–734.

[14] M. Ziegmann and F.H. Frimmel, *Photocatalytic degradation of clofibric acid, carbamazepine and iomeprol using conglomerated TiO_2 and activated carbon in aqueous suspension*, Water Sci. Tech. 61(1) (2010), pp. 273–281.

[15] R. Ocampo-Pérez, M. Sánchez-Polo, J. Rivera-Utrilla, and R. Leyva-Ramos, *Enhancement of the catalytic activity of TiO_2 by using activated carbon in the photocatalytic degradation of cytarabine*, Appl. Catal., B. 104 (2011), pp. 177–184.

[16] T.-T. Lim, P.-S. Yap, M. Srinivasan, and A.G. Fane, *TiO_2/AC composites for synergistic adsorption-photocatalysis processes: Present challenges and further developments for water treatment and reclamation*, Crit. Rev. Environ. Sci. Technol. 41 (2011), pp. 1173–1230.

[17] J. Matos, A. Garcia, T. Cordero, J.-M. Chovelon, and C. Ferronato, *Eco-friendly TiO_2-AC photocatalyst for the selective photooxidation of 4-chlorophenol*, Catal. Lett. 130 (2009), pp. 568–574.

[18] A.G. Thomas, W.R. Flavell, A.K. Mallick, A.R. Kumarasinghe, D. Tsoutsou, N. Khan, C. Chatwin, S. Rayner, C.G. Smith, R.L. Stockbauer, S. Warren, T.K. Johal, S. Patel, D. Holland, A. Taleb, and E. Wiame, *Comparison of the*

electronic structure of anatase and rutile TiO_2 single-crystal surfaces using resonant photoemission and X-ray absorption spectroscopy, Phys. Rev. B: Condens. Matter Mater. Phys. 75 (2007), pp. 035105-1–035105-12.

[19] J. Matos, J. Laine, J.-M. Herrmann, D. Uzcategui, and J.L. Brito, *Influence of activated carbon upon titania on aqueous photocatalytic consecutive runs of phenol photodegradation*, Appl. Catal., B 70 (2007), pp. 461–469.

[20] T. Cordero, J.-M. Chovelon, C. Duchamp, C. Ferronato, and J. Matos, *Surface nano-aggregation and photocatalytic activity of TiO_2 on H-type activated carbons*, Appl. Catal., B 73 (2007), pp. 227–235.

[21] B. Legube, M. Doré, B. Langlais, M.M. Bourbigot, and G. Gouesbet, *Changes in the chemical nature of a biologically treated wastewater during disinfection by ozone*, Ozone: Sci. Eng. 9 (1987), pp. 63–84.

[22] L.B. Clark, R.T. Rosen, T.G. Hartman, L.H. Alaimo, J.B. Louis, C. Hertz, C.-T. Ho, and J.D. Rosen, *Determination of nonregulated pollutants in three New Jersey publicly owned treatment works (POTWs)*, Res. J. Water Pollut. C 63 (1991), pp. 104–113.

[23] J.A. Pedersen, M.A. Yeager, and I.H. Suffet, *Xenobiotic organic compounds in runoff from fields irrigated with treated wastewater*, J. Agric. Food Chem. 51 (2003), pp. 1360–1372.

[24] H. Gulyas, M. Reich, and I. Sekoulov, *Characterization of a biologically treated wastewater from oil reclaiming: Recording of low molecular weight organics and estimation of humic substances*, Water Sci. Technol. 29 (9) (1994), pp. 195–198.

[25] H. Gulyas, and M. Reich, *Organic constituents of oil reclaiming wastewater*, J. Environ. Sci. Health, Part A: Toxic/Hazard. Subst. Environ. Eng. 35 (2000), pp. 435–464.

[26] Normenausschuss Wasserwesen, German standard methods for the examination of water, waste water and sludge; general measures of effects and substances (group H); Determination of total organic carbon (TOC) (H 3) (in German), DIN EN 1484 (1997–08), DIN Deutsches Institut für Normung e.V., Berlin, 1997.

[27] M. Abert, *LC-OCD-OND analysis of sewage treatment steps*. Karlsruhe, Germany: DOC-Labor Dr. Huber, Analytical Services and LC–OCD Systems; 2008. Available at http://www.doc-labor.de/html/Example_Report_WASTE.pdf (accessed September 2012).

[28] H. Kawaguchi, *Photocatalytic decomposition of phenol in the presence of titanium dioxide*, Environ. Technol. Lett. 5 (1984), pp. 471–474.

[29] A. Ortiz-Gomez, B. Serrano-Rosales, and H. de Lasa, *Enhanced mineralization of phenol and other hydroxylated compounds in a photocatalytic process assisted with ferric ions*, Chem. Eng. Sci. 63 (2008), pp. 520–557.

[30] E. Diamadopoulos, P. Samaras, and G.P. Sakellaropoulos, *The effect of activated carbon properties on the adsorption of toxic substances*, Water Sci. Technol. 25(1) (1992), pp. 153–160.

[31] A. Albert and E.P. Serjeant, *Ionization constants of acids and bases: A laboratory manual*, Methuen, London, 1962.

[32] L. Gu, Z. Chen, C. Sun, B. Wei, and X. Yu, *Photocatalytic degradation of 2,4-dichlorophenol using granular activated carbon supported TiO_2*, Desalination 263 (2010), pp. 107–112.

[33] L.F. Velasco, I.M. Fonseca, J.B. Parra, J.L. Lima, and C.O Ani, *Photochemical behaviour of activated carbons under UV irradiation*, Carbon 50 (2012), pp. 249–258.

[34] H. Gulyas, P. Choromanski, N. Muelling, and M. Furmanska, *Toward chemical-free reclamation of biologically pretreated greywater: Solar photocatalytic oxidation with powdered activated carbon*, J. Clean. Prod. 17 (2009), pp. 1223–1227.

[35] B. Zhu and L. Zhou, *Trapping and decomposing of color compounds from recycled water by TiO_2 coated activated carbon*, J. Environ. Manage. 90 (2009), pp. 3217–3225.

[36] H. Gulyas, K. Hartrampf, I.J. Ilesanmi, Z. Mahmood, W.-A. Storm, A.L. Susanto, R. Otterpohl, F. Köneke, M. Furmanska, K. Harasiuk, and I. Krawczyk, *Study of parameters affecting photocatalytic oxidation of biologically treated greywater*, Solar World Congress, Orlando, Florida, August 6–12, 2005. Available at http://www.tu-harburg.de/t3resources/aww/publikationen/pdf/GulyasSWCOrlando2005.pdf (accessed September 2012).

[37] G. Xue, H. Liu, Q. Chen, C. Hills, M. Tyrer, and F. Innocent, *Synergy between surface adsorption and photocatalysis during degradation of humic acid on TiO_2/activated carbon composites*, J. Hazard. Mater. 186 (2011), pp. 765–772.

[38] P.-S. Yap and T.-T. Lim, *Solar regeneration of powdered activated carbon impregnated with visible-light responsive photocatalyst: Factors affecting performances and predictive model*, Water Res. 46 (2012), pp. 3054–3064.